CHAPTER IV
EFFECT OF DIETARY POSTBIOTIC LIC37 ON LIVER TRANSCRIPTOMIC PROFILE OF CALVES

4.1 Abstract

This study aimed to investigate the effect of postbiotic from heat killed *Limosilactobacillus ingluviei* C37 (postbiotic LIC37) on liver transcriptional response of calves. Fourteen calves were assigned to 2 treatment groups: CON (n = 7) or TRT (n = 7, fed 108 CFU/d of inactivated Lactobacillus ingluviei CR37 strain). Calves received milk replacer (MR) at 1.75% of body weight (based on air-dry weight) and the amount was adjusted weekly according to body weight, while fresh and clean water was provided ad libitum. All calves had free access to starter feed starting on day 33. On day 82, the MR solution was reduced to 50% of the previous week's allocation, and calves were completely weaned by day 89. Liver samples were collected after slaughter on day 90. Transcriptome analysis identified 33 DEGs, including 16 upregulated DEGs such as Endothelial lipase (LIPG), Peroxisomal Acyl-CoA oxidase 1 (ACOX1), Solute carrier family 27 member 6 (SLC27A6), and 17 downregulated DEGs such as Family with sequence similarity 107 member A (FAM107A), 4-Hydroxy-2-oxoglutarate aldolase 1 (HOGA1), Farnesyl diphosphate synthase (FDPS). Kyoto Encyclopedia of Genes and Genomes (KEGG) analysis identified 11 significant pathways, including the PPAR signaling pathway and Pentose phosphate pathway. Taken together, postbiotic LIC37 supplementation demonstrated potential benefits in improving lipid metabolism and mitigating oxidative stress in weaning calves.

Keywords: Postbiotic, *Limosilactobacillus*; Calf weaning; Transcriptome; Liver; lipid metabolisms.

4.2 Introduction

Weaning is a critical and demanding transition for calves, frequently leading to physiological stress responses and disrupting energy homeostasis (Agustinho et al., 2024), which can compromise growth performance and overall health. As a key regulatory hub for overall energy metabolism, the liver plays a pivotal role in metabolic adaptation by modulating fatty acid uptake and release, de novo synthesis, and lipid utilization through β-oxidation, and oxidative stress responses (Badmus et al., 2022).

During weaning, nutrient intake of calves is insufficient, and ammonia absorbed by the rumen increases the burden on the liver through the liver urea cycle (Laarman et al., 2012; Batista et al., 2022). Additionally, excessive lipid accumulation in the liver exacerbates oxidative stress, enhances fatty acid oxidation, and triggers the release of proinflammatory cytokines, which collectively contribute to mitochondrial and hepatocyte damage, inflammation, and the activation of fibrotic pathways (Kutlu et al., 2018).

Dietary intervention optimizes energy balance by enhancing antioxidant defense and regulating lipid metabolism, offering a new approach to alleviate weaning stress in calves. Probiotics are defined as a "preparation of inanimate microorganisms and/or their components that confers a health benefit on the host" (Salminen et al., 2021). In recent years, postbiotics, as an alternative to probiotics, have been extensively used to improve growth and lactation performance, as well as to enhance immunity and antioxidant defenses (Stefańska et al., 2022; Chae et al., 2024). For example, Ríus et al. (2022) reported postbiotic from *Aspergillus oryzae* improved energy-use efficiency in calves exposed to heat stress. Similarly, Dai et al. (2024) demonstrated that supplementing transition dairy cows with postbiotics from *Saccharomyces cerevisiae* could be beneficial for improving liver metabolism. Additionally, Izuddin et al. (2020) observed that the antioxidant enzymes concentration were increased by postbiotic *Lactobacillus plantarum* in post-weaning lambs. However, the molecular mechanisms through which postbiotics influence liver metabolism in weaned calves remain to be investigated. Recently, RNA-Seq technology efficiently identifies nearly all transcripts in tissue, thereby uncovering the molecular mechanisms underlying biological phenomena (Malone and Oliver, 2011).

4.3 Objective

This study aimed to investigate the effects of postbiotics from heat killed *Limosilactobacillus ingluviei* C37 on growth performance, antioxidant capacity, and liver transcriptomics in calves during the weaning period.

4.4 Materials and methods

4.4.1 Ethics statement

The experiments were carried out at the Suranaree University of Technology (SUT) farm according to the approved protocol by the Animal Care and Use Committee of SUT, Thailand (document no. SUT-IACUC-0020/2023).

4.4.2 Animals, treatment and sampling method

The *Limosilactobacillus ingluviei* C37 strain was obtained from the Laboratory of Monogastric Animal Nutrition and Feed Science at Suranaree University of Technology (SUT). The isolation and cultivation of *L. ingluviei* C37 were thoroughly detailed by Sirisopapong et al. (2023). The inactivated preparation of *L. ingluviei* C37 was achieved by heat-killing the cells at 80°C for 30 minutes, following the method described by Tsukagoshi et al. (2020).

Fourteen Holstein bull calves were obtained from a local dairy farm at the age of 5.71 ± 1.14 d. Each calf received 2 liters of colostrum within 3 hours of birth, followed by an additional 2 liters within the next 12 hours. All calves with serum total protein levels exceeding 5.6 g/dL at 24 hours of birth were selected, confirming the successful transfer of passive immunity (Hernandez et al., 2016). The calves were gradually transitioned from colostrum to bucket-fed milk replacer (MR) beginning at three days of age before being transferred to the SUT farm. Upon arrival, they received an immediate intramuscular injection of vitamin B12 (Catosal^{TM}, OLIC Co. Ltd, Ayutthaya, Thailand) at a 5% (mL/kg) dosage. All calves were blocked into 2 groups by body weight (37.34 ± 3.19 kg, and 28.83 ± 2.92 kg; mean ± SD), and randomly assigned to 2 treatments (7 per treatment). Namely, CON group (without postbiotic) and TRT group with 1 g/d of postbiotic LIC37 (10^8 CFU/g). The dosage was determined based on conversions from previous studies (Thorsteinsson et al., 2020; McNeil et al., 2024). Each calf was kept in an individually pen (2.2 m × 2.4 m) equipped with rubber mats

and wood pellets. The soiled wood pellets were removed daily, and fresh wood pellet was provided weekly.

Commercial MR was procured from Dairy-Rich Co. Ltd (Bangkok, Thailand), with its nutrient composition detailed in **Table 3.1** (Chapter III). The MR for calves was provided twice daily at 08:00 and 16:00 at a concentration of 15%, equivalent to 1.75% of BW (base on air-dry). The feeding amount was adjusted weekly based on BW. The postbiotic was mixed into the morning MR feeding, while fresh and clean water was available *ad libitum*. As the sole solid feed, the commercial starter (Charoen Pokphand Foods, Bangkok, Thailand) was provided *ad libitum* from day 33 of the experiment.

The 90-day feeding trial began on the day the calves arrived at SUT farm. The weaning process was completed within one week. Specifically, it started on day 82, with the MR solution reduced to 50% of the previous week's allocation. Calves were completely weaned by day 89. This feeding strategy was intended to induce weaning stress (Van Niekerk et al., 2021). On day 90, prior to the morning feeding, all calves were euthanized by captive bolt stunning and exsanguination. The liver tissue was taken from the caudate lobe into sterile RNase-free tubes, snap-frozen in liquid nitrogen, and then stored at -80°C for future RNA extraction.

4.4.3 RNA extraction and RNA-seq library construction

According to the manufacturer`s instructions, total RNA was obtained from liver tissue using TRIzol reagent (Molecular Research Center, Cincinnati, Ohio, USA). The quality and quantity of the extracted RNA were analyzed using spectrophotometry (NanoDrop 2000 spectrophotometer, Thermo Fisher Scientific, Waltham, MA, USA) and assessed by 1% agarose (w/v) gel electrophoresis, with 0.5 × TAE buffer and an applied electric current of 100 V for 20 minutes. RNA integrity was further evaluated using capillary electrophoresis on the QIAxcel Connect (Qiagen) to determine the RNA integrity number (RIN). RNA samples with a RIN > 8 were selected for the construction of RNA libraries.

RNA reverse transcription, library preparation, and RNA sequencing (RNA-seq) were carried out at BGI Co., Ltd. (Shenzhen, China). Briefly, total RNA was enriched for mRNA by poly(A) selection using oligo(dT) magnetic beads, followed by reverse transcription and cDNA synthesis. The resulting double-stranded cDNA underwent end repair, 5'-phosphorylation, and 3'-adenylation to prepare for adapter ligation. The adapter-ligated products were then PCR amplified, denatured, and circularized using bridging

primers to create single-stranded circular DNA libraries. Sequencing was performed on the DNBSEQ platform with PE500 (BGI Co., Ltd., Shenzhen, China). The raw sequencing data were processed using SOAPnuke (v1.5.6, RRID:SCR_015025) to eliminate low-quality and adapter-contaminated reads. The filtering criteria were as follows: 1) removal of reads containing adapter sequences, 2) exclusion of reads with more than 5% unknown bases (N), and 3) discarding low-quality reads, defined as those in which more than 20% of the bases had a quality score below 15.

4.4.4 Transcriptome sequencing, data analysis, and functional enrichment analyses

The high-quality reads were retained as clean data and subsequently analyzed using the online multi-omics data mining platform (biosys.bgi.com). In brief, The sequencing reads were mapped to the *Bos taurus* reference genome (GeneBank Assembly ID: GCA_002263795.2) using HISAT2 (version 2.2.1) with default settings (Kim et al., 2015). Cleaned data were then aligned to the reference transcriptome using Bowtie (version 2.3.4.3) (Langmead and Salzberg, 2012). Gene expression levels were quantified with RSEM (version 1.3.1) (Li and Dewey, 2011). Differential gene expression analysis between the two groups was performed using DESeq2 (version 1.4.5) (Love et al., 2014). The transcripts were filtered for sufficient normalized read depth, requiring transcripts per million greater than 0 (TPM > 0) in at least 5 samples per group.

Transcripts with a fold-change (FC) of ≥ 1 and an adjusted P value < 0.05 were considered differentially expressed genes (DEGs). Gene Ontology (GO) annotation and Kyoto Encyclopedia of Genes and Genomes (KEGG) pathway enrichment analyses for DEGs were performed using the Phyper function in R software. GO terms and KEGG pathways with a P value < 0.05 were performed regarded as significantly enriched. All sequencing data have been deposited in the Gene Expression Omnibus (GEO) of the National Center for Biotechnology Information (NCBI) database under the accession number GSE293736.

4.4.5 Quantitative polymerase chain reaction to validate DEGs

To confirm the reliability and precision of gene expression data obtained from RNA-Seq, quantitative PCR (qPCR) was conducted on the same RNA samples. The RNA was reverse transcribed into cDNA using SweScript All-in-One RT SuperMix (G3337, Servicebio Technology Co., Ltd., Wuhan, China) according to the manufacturer's instructions. Using Primer3 software (https://primer3.ut.ee/) designed primers (**Table 4.1**), and subsequently

synthesized by Servicebio Technology Co., Ltd. (Wuhan, China). Five target genes were Endothelial lipase (LIPG), Acyl-CoA oxidase 1 (ACOX1), Family with sequence similarity 107 member A (FAM107A), 4-Hydroxy-2-Oxoglutarate aldolase 1 (HOGA1), and Farnesyl diphosphate synthase (FDPS). Glyceraldehyde-3-phosphate dehydrogenase (GAPDH) was housekeeping gene in this study. The qPCR was performed on CFX Connect™ Real-Time PCR System (Bio-Rad, California, USA) in a reaction solution (15 μL) contained 2 μL of cDNA template, 1.5 μL of each primer (10 μM), 7.5 μL of 2×Universal Blue SYBR Green qPCR Master Mix (G3326, Wuhan Servicebio Technology Co., Ltd), and 4 μL of nuclease-free water. The qPCR conditions were as follows: predegeneration at 95℃ for 30 seconds, followed by 40 cycles of denaturation at 95℃ for 15 seconds, annealing at 60℃ for 15 seconds, and extension at 60℃ for 30 seconds. Relative expression levels were determined using the $2^{-\Delta\Delta CT}$ method (Love et al., 2014), and the resulting values were transformed into fold change (FC) to enable comparison with RNA-Seq data.

Table 4.1 Primer sequences used in quantitative PCR.

Gene	Primer sequences (5' to 3')	Accession
LIPG	(F): TCA AGC CCC TTC ACA TTC CC	XM_002697766
	(R): CTC TCG AAG TTT CCA GCG GT	
ACOX1	(F): GCG TTA CGA GGT GGC TGT TA	NM_001035289
	(R): GGC CCA CAG GTT CCA CAA AA	
FAM107A	(F): CTG AGA ACG CAG GAC CCG	XM_024982918
	(R): AGC AGC TTC TTG GGC TTG AT	
HOGA1	(F): GAG GTG GAC TAT GGG AAA CTG G	XM_024985530
	(R): CCT CTG AAC TTC TCT TGC CTG T	
FDPS	(F): GAG GCA GGG GCT AGA AAC TC	XM_024984593
	(R): ATT CCC AAA ACG GGG GAA CA	

LIPG, Endothelial lipase; ACOX1, Peroxisomal Acyl-CoA oxidase 1; FAM107A, Family with sequence similarity 107 member A; HOGA1, 4-hydroxy-2-oxoglutarate aldolase 1; FDPS, Farnesyl diphosphate synthase.

4.5 Results

4.5.1 RNA-Seq data processing and quality control

According to the results presented in **Table S4.1**. RNA sequencing generated an average of 46.82 million raw reads from 14 libraries, with minimum of 45.44 million to a maximum of 47.19 million. After quality control, an average of 45.03 million clean reads were obtained, with the number of clean reads ranging from a minimum of 43.84 million to a maximum of 45.51 million. A minimum of 95.74% of the reads demonstrated a sequence quality score above Q30. The total Mapping rates ranged from 98.29% to 98.66%, and the average unique mapping rate was 95.01%.

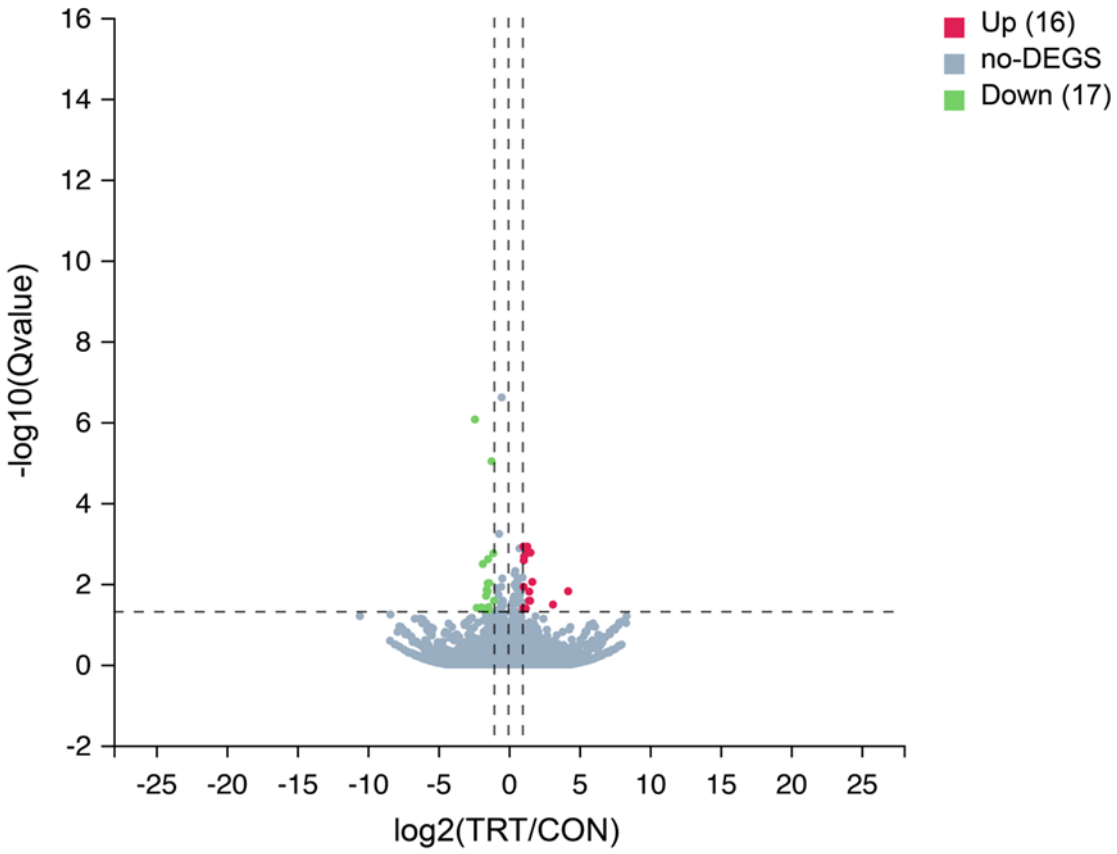

Figure 4.1 Volcano plot of differentially expressed genes in the liver tissue of calves. The red and green dots representing upregulated and downregulated transcripts, respectively. Gray dots represent insignificant DEGs. The x and y axes of the volcano plots show the log2 fold changes and –log10 q value, respectively.

4.5.2 Detection of DEGs

As presented in **Figure 4.1**. A total of 33 DEGs were identified in liver tissue, with 16 upregulated and 17 downregulated transcripts. Detailed information about the identified DEGs is provided in **Table S 4.2**.

Among these, Endothelial Lipase (LIPG), Peroxisomal Acyl-CoA oxidase 1 (ACOX1), Solute carrier family 27 member 6 (SLC27A6), Elongation of very long chain fatty acids protein 6 (ELOVL6), Glycerate kinase (GLYCTK), 4-Hydroxy-2-oxoglutarate aldolase 1 (HOGA1), Exostosin like glycosyltransferase 1 (EXTL1), and Farnesyl diphosphate synthase (FDPS) were indentified. The top 10 upregulated and down regulated DEGs shown in **Table 4.2**.

Table 4.2 Top 10 upregulated and downregulated differentially expressed genes in the liver tissue of calves.

Gene ID	Gene Symbol	log2 fold change	Qvalue[1]	Regulated[2]
509808	LIPG	4.22	0.0155	Up
781161	FREM3	3.14	0.0330	Up
513996	ACOX1	1.69	0.0092	Up
537062	SLC27A6	1.55	0.0017	Up
613923	DYM	1.53	0.0266	Up
533333	ELOVL6	1.47	0.0158	Up
534842	ROBO2	1.45	0.0266	Up
524334	L3MBTL3	1.34	0.0016	Up
507949	GLYCTK	1.32	0.0012	Up
525346	NCOA1	1.22	0.0414	Up
538515	FAM107A	-2.38	0.0000	Down
506001	HOGA1	-2.25	0.0397	Down
782061	LOC782061	-1.92	0.0387	Down
281156	FDPS	-1.83	0.0033	Down
505584	FXYD5	-1.68	0.0444	Down
785762	DDH3	-1.60	0.0448	Down

Table 4.2 Continue.

Gene ID	Gene Symbol	log2 fold change	Qvalue[1]	Regulated[2]
112442367	-	-1.59	0.0202	Down
786492	LGALS3	-1.55	0.0143	Down
507550	-	-1.47	0.0155	Down
281240	IGF2	-1.47	0.0099	Down

[1] LIPG, Endothelial lipase; FREM3, FRAS1 related extracellular matrix protein 3; ACOX1, Peroxisomal Acyl-CoA oxidase 1; SLC27A6, Solute Carrier Family 27 Member 6; DYM, Dymeclin; ELOVL6, Elongation of very long chain fatty acids protein 6; ROBO2, Roundabout guidance receptor 2; L3MBTL3, L3MBTL transcriptional repressor 3; GLYCTK, Glycerate kinase; NCOA1, Nuclear receptor coactivator 1; FAM107A, Family with sequence similarity 107 member A; HOGA1, 4-hydroxy-2-oxoglutarate aldolase 1; LOC782061, Aldo-keto reductase family 1, member C1-like; FDPS, Farnesyl diphosphate synthase; FXYD5, FXYD domain containing ion transport regulator 5; DDH3, Dihydrodiol dehydrogenase 3; LGALS3, Galectin 3; IGF2, Insulin-like growth factor 2.

[2] Q value is adjusted of P value.

4.5.3 GO and KEGG pathway enrichment of DEGs

Gene Ontology (GO) analysis categorized these DEGs into three functional groups: biological processes (BP), molecular functions (MF), and cellular components (CC). Specifically, the significant DEGs were annotated into 50 CC terms, among which 12 were significantly enriched (**Figure 4.2**). Additionally, they were mapped to 193 BP terms, with 116 showing significant enrichment (**Figure 4.2**), and 97 MF terms, of which 50 were significantly enriched (**Figure 4.3**).

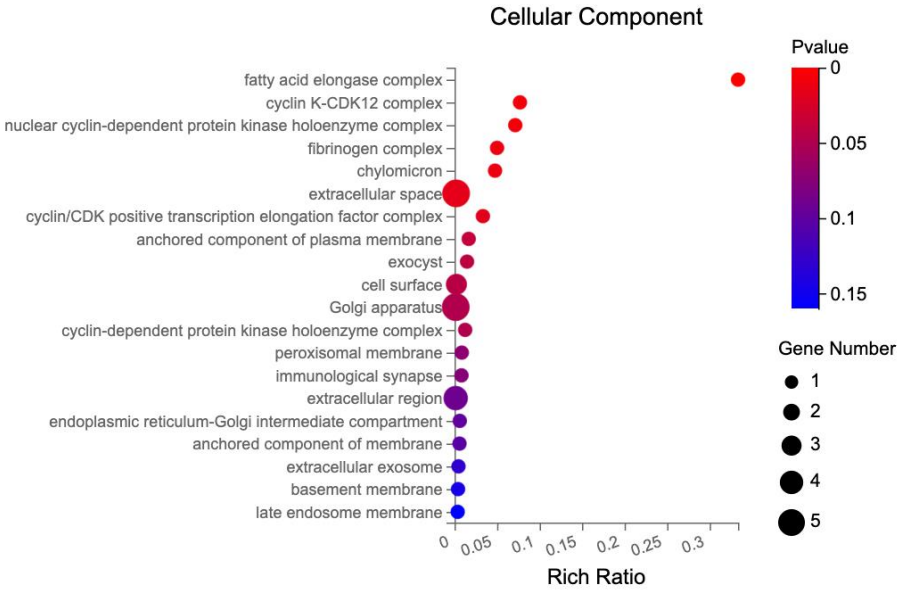

Figure 4.2 Top 20 GO cellular component terms enriched in differentially expressed genes in liver tissue in calves. The circle size in each term corresponds to the number of genes. The circle's color goes from blue to red, indicating a lower P value.

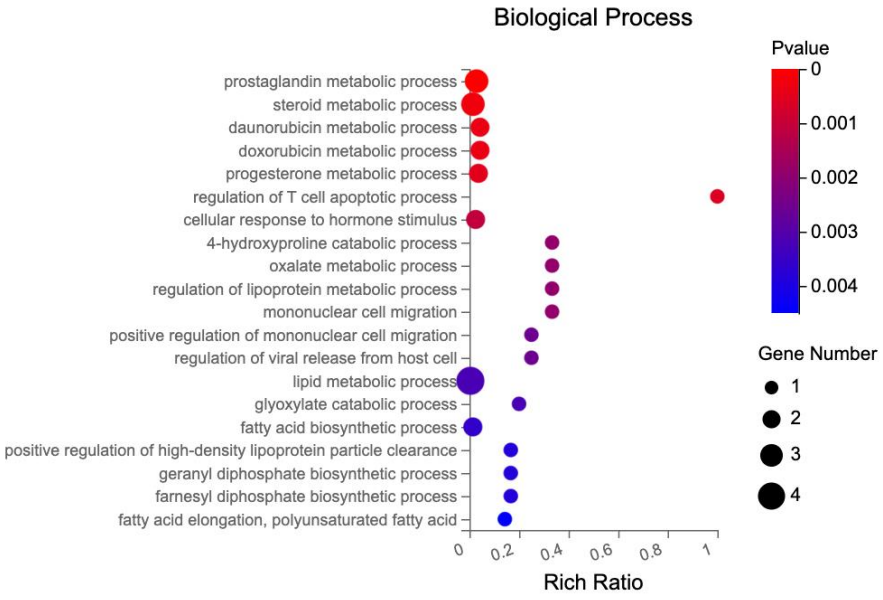

Figure 4.3 Top 20 GO biological process terms enriched in differentially expressed genes in liver tissue in calves.

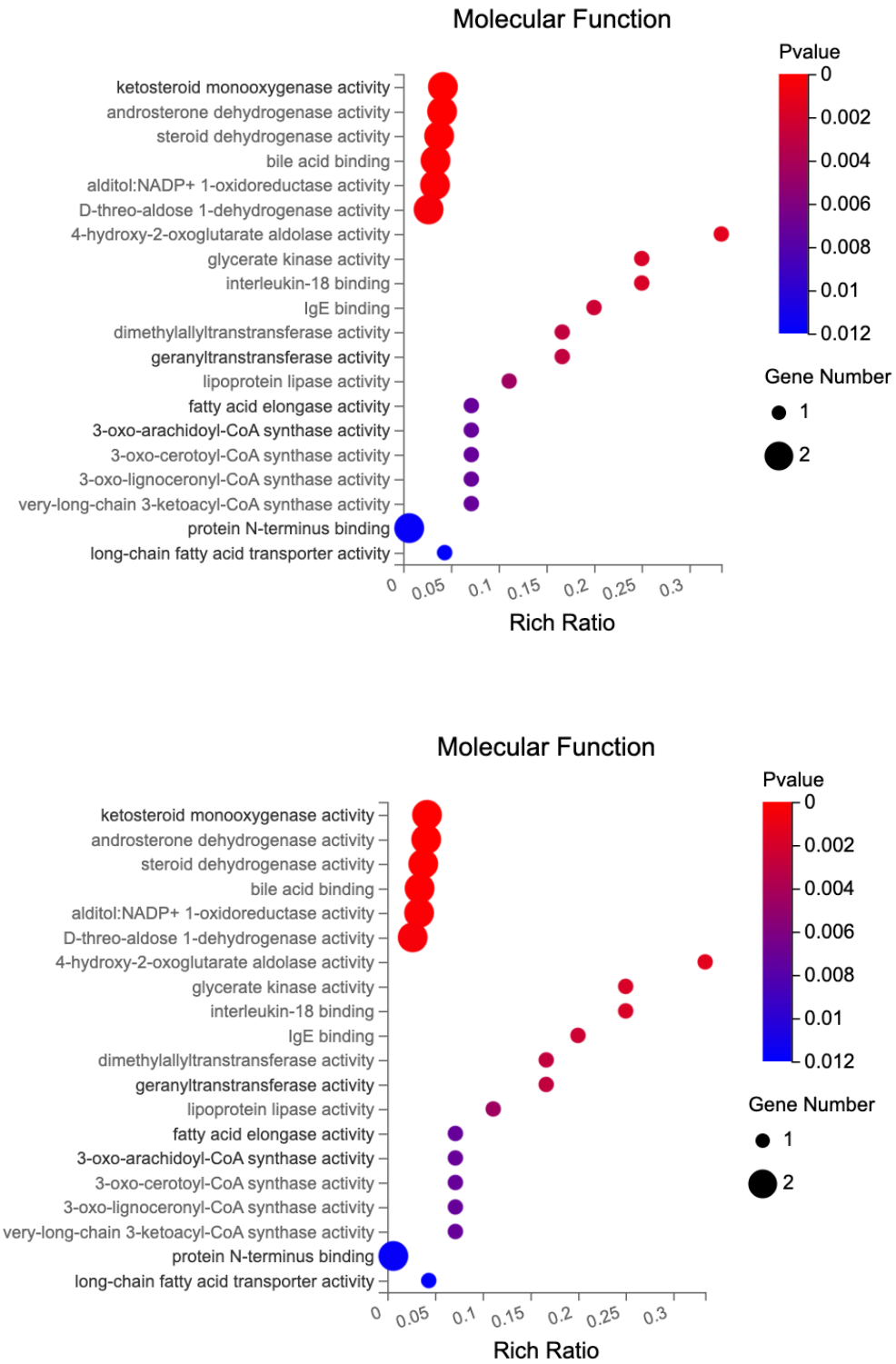

Figure 4.4 Top 20 GO Molecular function terms enriched in differentially expressed genes in liver tissue in calves.

A total of 47 KEGG pathways were identified from 33 DEGs, among which 11 pathways were significant enriched (**Table 4.3**). These include the PPAR signaling pathway (bta03320, P = 0.0109), Fatty acid metabolism (bta01212, P = 0.0037), Carbon metabolism (bta01200, P = 0.0105), Biosynthesis of unsaturated fatty acids (bta01040, P = 0.0005), Terpenoid backbone biosynthesis (bta00900, P = 0.0294), Glyoxylate and dicarboxylate metabolism (bta00630, P = 0.0007), alpha-Linolenic acid metabolism (bta00592, P = 0.0357), Glycerolipid metabolism (bta00561, P = 0.0058), Glycosaminoglycan biosynthesis - heparan sulfate / heparin (bta00534, P = 0.0315), Fatty acid elongation (bta00062, P = 0.0310), and the Pentose phosphate pathway (bta00030, P = 0.0456).

Table 4.3 Kyoto encyclopedia of genes and genomes pathways possibly affected by postbiotic in liver tissue of calves.

Pathway Term	Count	P value	Gene Symbols[1]
bta03320: PPAR signaling pathway	2	0.0109	ACOX1↑, SLC27A6↑
bta01212: Fatty acid metabolism	2	0.0037	ACOX1↑, ELOVL6↑
bta01200: Carbon metabolism	2	0.0105	ACOX1↑, GLYCTK↑
bta01040: Biosynthesis of unsaturated	2	0.0005	ACOX1↑, ELOVL6↑
bta00900: Terpenoid backbone	1	0.0294	FDPS↓
bta00630: Glyoxylate and	2	0.0007	GLYCTK↑, HOGA1↓
bta00592: alpha-Linolenic acid	1	0.0357	ACOX1↑
bta00561: Glycerolipid metabolism	2	0.0058	LIPG↑, GLYCTK↑
bta00534: Glycosaminoglycan	1	0.0315	EXTL1↓
bta00062: Fatty acid elongation	1	0.0310	ELOVL6↑
bta00030: Pentose phosphate	1	0.0456	GLYCTK↑

Up and down arrows indicate the upregulated and downregulated genes, respectively, in liver tissue of calves fed postbiotic LIC37.

4.5.4 qPCR validated RNA-seq results

We validated the expression levels of five transcripts, including two upregulated transcripts (e.g. ACOX1 and LIPG) and three downregulated transcripts (e.g. FAM107A, HOGA1, and FDPS), were quantified in liver tissue. All transcripts showed similar

expression trends in both qPCR and RNA-seq (**Figure 4.3**). These results validate the accuracy of the identified transcripts and support the reliability of the RNA-seq results.

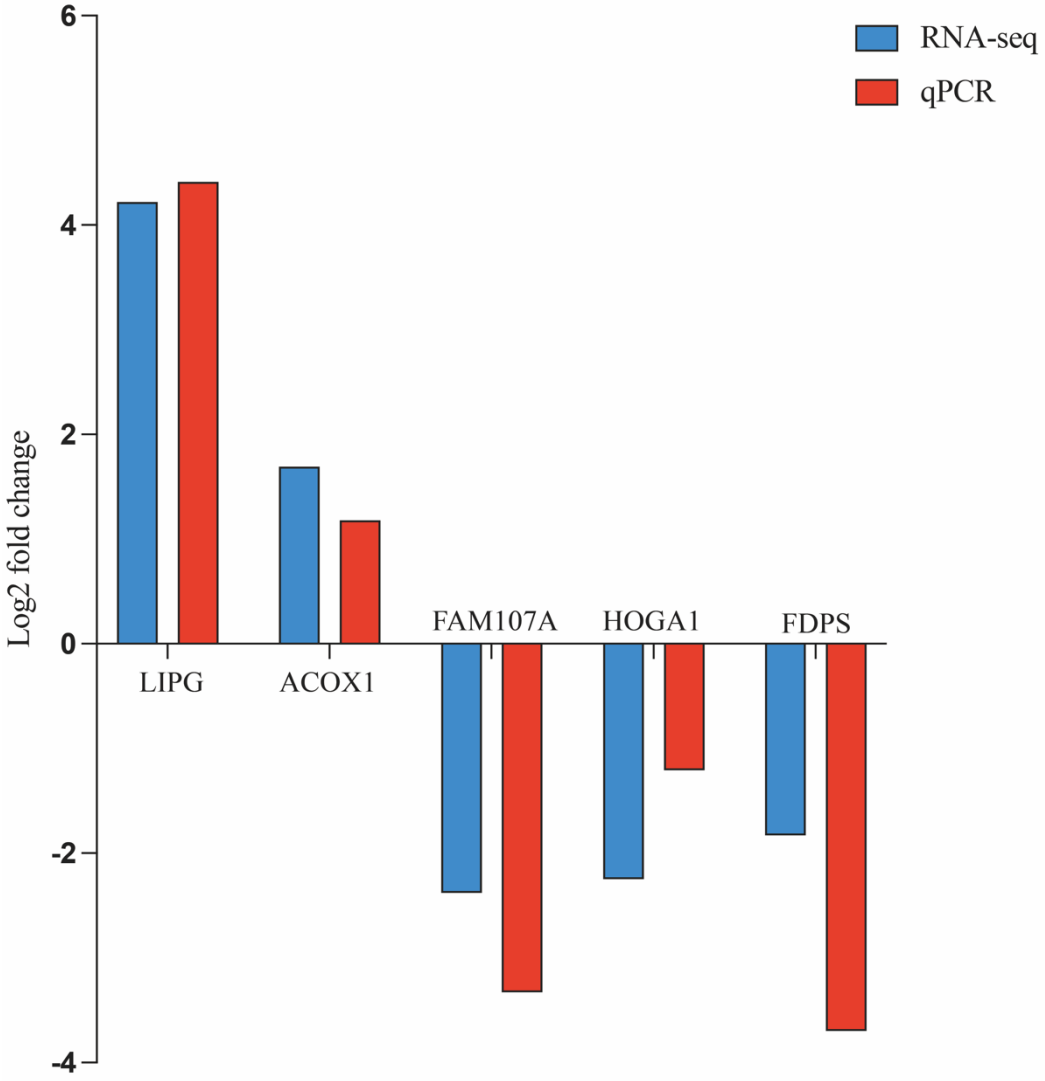

Figure 4.5 Quantitative PCR (qPCR) was employed to validate five DEGs in RNA-seq analysis. The x-axis denotes the genes, while the y-axis shows their mRNA expression levels as fold-change (FC) values. Expression levels obtained from RNA-seq and qPCR are illustrated by blue and red bars, respectively. LIPG, Endothelial lipase; ACOX1, Peroxisomal Acyl-CoA oxidase 1; FAM107A, Family with sequence similarity 107 member A; HOGA1, 4-hydroxy-2-oxoglutarate aldolase 1; FDPS, Farnesyl diphosphate synthase.

4.6 Discussion

LIPG, ACOX1, and SLC27A6 are key regulators of lipid metabolism, contributing to fatty acid hydrolysis, oxidation, and transport. These genes contribute collectively to lipid homeostasis and energy metabolism. LIPG, a member of the triglyceride lipase family, is one of the key regulators of glyceride hydrolysis while directly facilitating the release of free fatty acids from phospholipids (Zhou et al., 2021) and high density lipoproteins (Strauss et al., 2003), playing a crucial role in maintaining cell structure, regulating cytokine expression, and providing energy (Hong et al., 2021). In the present study, LIPG expression in the TRT group had a FC of 4.22 greater than the CON group, suggesting that postbiotic LIC37 potentially enhanced glyceride hydrolysis and increased the release of free fatty acids. This may imply that postbiotic potentially enhances lipid mobilization and contributes to energy homeostasis in weaned calves.

ACOX1 is an essential enzyme in the acyl-CoA oxidase family and a key rate-limiting enzyme in peroxisomal β-oxidation (Shi et al., 2025). It facilitates the degradation of long-chain, branched-chain, and medium-chain fatty acids by promoting peroxisomal β-oxidation (He et al., 2020). The upregulation of ACOX1 in the TRT group observed in the present study suggests that postbiotic LIC37 may activate peroxisomal β-oxidation, which in turn promotes fatty acid degradation and enhances liver energy production in weaned calves. This result is consistent with previous finding by Wang et al. (2019), who demonstrated that *L. frumenti* administration upregulated ACOX1 protein, highlighting its role in activating fatty acid β-oxidation in the liver of early-weaned piglets. Thus, the upregulation of ACOX1 suggests a beneficial effect of postbiotic LIC37 on fatty acid metabolism, which may support the energy demands during the weaning process.

SLC27A6, is a member of the fatty acid transport family, and plays specific roles in fatty acid homeostasis (Bonen et al., 2007). As a membrane-associated fatty acid-binding protein, it regulates fatty acid transport, thereby influencing its utilization for triglyceride synthesis within the cell (Zhang et al., 2021). Additionally, SLC27A6 impacts lipid accumulation in tissues and cells by modulating fatty acid lipidation and oxidation (Huang et al., 2021). This finding is in line with previous reports by Nafikov et al. (2013), who reported that increased SLC27A6 expression promoted the uptake of fatty acids from plasma and the intracellular transport of fatty acids by mammary epithelial cells.

Collectively, these findings indicate postbiotic LIC37 may promote fatty acid absorption and intracellular transport, potentially influencing lipid metabolism and energy distribution.

FDPS and HOGA1 are involved in lipid storage and adipogenesis. FDPS is a key enzyme involved in cholesterol and sterol biosynthesis (Claire D'Andre et al., 2013), playing a critical role in cholesterol and steroid metabolism by producing farnesyl diphosphate (Szkopiński and Płochocka, 2005). Downregulation of FDPS has been shown to suppress adipocyte differentiation in chickens (Zhu et al., 2023). The downregulation of FDPS inhibits intramuscular adipose differentiation and reduces energy storage, suggesting that postbiotic LIC37 may regulates energy redistribution in calves during weaning period. Similarly, HOGA1 is involved in glyoxylate and dicarboxylic acid metabolism, arginine and proline metabolism and other pathways to promote adipogenesis (Ye et al., 2024). Inhibition of HOGA1 has been shown to downregulate the expression of PPARγ, C/EBPα, AP2, CD36, and adiponectin during mouse adipocyte differentiation, thereby suppressing intracellular fat deposition (Kim et al., 2022). The downregulation of HOGA1 in the TRT group suggests that postbiotic LIC37 may inhibit adipogenesis and reduce liver fat accumulation, potentially shifting energy utilization away from lipid storage toward other metabolic processes.

FREM3 and FAM107A contribute to cell integrity and metabolic adaptation. FREM3 is a basement membrane protein of the Fras1-related extracellular matrix family, playing a crucial role in maintaining embryonic epithelial–mesenchymal integrity (Pavlakis et al., 2011). The upregulation of FREM3 by postbiotic LIC37 suggests that postbiotic LIC37 contributes to the maintenance of cell integrity. FAM107A has been shown to regulate the expression of CRYAB (Manigandan et al., 2021), which in turn modulates the CRYAB/PI3K/AKT signaling axis, a critical pathway involved in cell survival and metabolism (Ke et al., 2022). Ming and Zhang (2025) demonstrated that FAM107A depletion reduces CRYAB expression and increases PI3K and AKT phosphorylation, while FAM107A overexpression disrupts metabolic processes, decreasing glucose uptake, lactate production, and ATP levels. The downregulation of FAM107A in the TRT group observed in this study may suggest that postbiotic LIC37 supplementation enhances cellular metabolism, improving glucose uptake and ATP levels, thereby alleviating the insufficient energy supply in calves during weaning.

FXYD5 is implicated in inflammation and extracellular matrix regulation. As a type I plasma membrane protein, can promotes inflammation through TNFα signaling in normal cells (Lubarski-Gotliv et al., 2016). Its expression is associated with cytoskeletal reorganization (Schüler et al., 2012), altered cell shape (Shimamura et al., 2004), and the disruption of tight and adherence junctions (Miller and Davis, 2008; Lee et al., 2012). Furthermore, increased FXYD5 expression may exacerbate inflammation, oxidative stress, and extracellular matrix degradation by activating the NF-**K**B signaling pathway (Song et al., 2022). In the present study, a lower expression of FXYD5 in the TRT group compared with CON group, suggests a potential associated with a reduction in inflammation, oxidative stress, and extracellular matrix degradation during the weaning process in calves. This reduction in FXYD5 expression may indicate a less severe inflammatory response, lower oxidative stress levels, and improved tissue integrity in the TRT group. This finding is further supported by the observed increase in plasma antioxidant enzyme activity.

At the transcriptomic level, activation of the PPAR signaling pathway plays a crucial role in fatty acid biosynthesis and metabolism (Zhou et al., 2016), the maintenance of energy balance (Dupont et al., 2012), and the regulation of fatty acid oxidation (Nakagawa et al., 2016). Xu et al. (2022) found that glycyrrhizic acid and compound probiotics improved intestinal fat digestion and absorption by regulating PPAR signaling pathway in weaned piglets. Similarly, Cao et al. (2019) demonstrated that *L. plantarum* WW fermented soybean extract could improve fatty liver in rats *via* PPAR signaling pathway. Additionally, Zang et al. (2024) suggested that PPAR may be a potential target of *Lactobacillus plantarum*, which exerts anti-inflammatory effects by binding to p65/p50 to inhibit NF-**K**B activity. Similarly, the present study indicates that the PPAR/ACOX1/SLC27A6 may serve as a key regulatory target of a postbiotic LIC37 in liver lipid metabolism. Specifically, the postbiotic upregulates the transcription of ACOX1 and SLC27A6 *via* activating PPAR signaling pathway. ACOX1 enhances β-oxidation, promoting lipid degradation to meet the metabolic energy demands of weaned calves, while SLC27A6, a fatty acid transport protein, facilitates the uptake and utilization of long-chain fatty acids, further optimizing energy supply. Besides, lipid metabolism-related pathways, including fatty acid metabolism, biosynthesis of unsaturated fatty acids, fatty acid elongation, which function in fatty acid modification,

elongation, and energy production. Furthermore, we found that the postbiotic LIC37 may regulate fatty acid production and energy supply by activating fatty acid metabolism, biosynthesis of unsaturated fatty acids, and fatty acid elongation pathways. Additionally, we found that DEGs were enriched in oxidative stress-related pathways such as alpha-linoleic acid metabolism, glycerolipid metabolism, glyoxylate and dicarboxylate metabolism, and pentose phosphate pathway. Among these, pentose phosphate pathway is the central glucose catabolic pathways that link glucose metabolism to ribose synthesis and NADPH production (Huang et al., 2019), providing reducing power to the glutathione antioxidant system to scavenge reactive oxygen species (ROS) and protect cells from oxidative damage (Winkler et al., 1986).

Overall, we speculated that postbiotic LIC37 may improve energy supply by regulating lipid metabolism through PPAR signaling pathway, fatty acid metabolism, biosynthesis of unsaturated fatty acids, and the fatty acid elongation. Additionally, the postbiotic may alleviate oxidative stress damage through activation of alpha-linoleic acid metabolism, glycerolipid metabolism, glyoxylate and dicarboxylate metabolism, and pentose phosphate pathway, thereby mitigating the negative effects of weaning stress on calves.

4.7 Conclusion

In conclusion, RNA-seq analysis showed that 33 DEGs with 16 upregulation and 17 downregulation. KEGG pathway analysis revealed 11 significantly enriched pathways, among which heat killed *Limosilactobacillus ingluviei* C37 may regulate lipid metabolism *via* PPAR signaling pathway, and mitigate oxidative stress through pentose phosphate pathway. These findings highlight the potential of heat killed *Limosilactobacillus ingluviei* C37 to improve lipid metabolism and alleviate oxidative stress in calves during weaning.

4.8 References

Agustinho, B., A. Wolfe, C. Tsai, L. Pereira, D. Konetchy, A. Laarman, and P. Rezamand. 2024. Effects of weaning age and pace on blood metabolites, cortisol concentration, and mRNA abundance of inflammation-related genes in

gastrointestinal, adipose, and liver tissue of Holstein dairy calves. **Journal of Dairy Science** 107(6):3988-3999. https://doi.org/10.3168/jds.2023-23642.

Badmus, Olufunto O., Sarah A. Hillhouse, Christopher D. Anderson, Terry D. Hinds, Jr., and David E. Stec. 2022. Molecular mechanisms of metabolic associated fatty liver disease (MAFLD): functional analysis of lipid metabolism pathways. **Clinical Science** 136(18):1347-1366. https://doi.org/10.1042/CS20220572.

Batista, C. P., R. S. Gonçalves, L. V. Q. Contreras, S. F. Valle, and F. González. 2022. Correlation between liver lipidosis, body condition score variation, and hepatic analytes in dairy cows. **Brazilian Journal of Veterinary Medicine** 44:e005121. https://doi.org/10.29374/2527-2179.bjvm005121.

Bonen, A., A. Chabowski, J. a. Luiken, and J. Glatz. 2007. Is membrane transport of FFA mediated by lipid, protein, or both? Mechanisms and regulation of protein-mediated cellular fatty acid uptake: molecular, biochemical, and physiological evidence. **Physiology** (Bethesda, Md.) 22:15-29. https://doi.org/10.1152/physiologyonline.2007.22.1.15.

Cao, C., R. Wu, X. Zhu, Y. Li, M. Li, F. An, and J. Wu. 2019. Ameliorative effect of Lactobacillus plantarum WW-fermented soy extract on rat fatty liver via the PPAR signaling pathway. **Journal of Functional Foods** 60:103439. https://doi.org/10.1016/j.jff.2019.103439.

Chae, J.-B., A. D. Schoofs, and J. L. McGill. 2024. Beneficial effects of Saccharomyces cerevisiae fermentation postbiotic products on calf and cow health and plausible mechanisms of action. **Frontiers in Animal Science** 5:1491970. https://doi.org/10.3389/fanim.2024.1491970.

Claire D'Andre, H., W. Paul, X. Shen, X. Jia, R. Zhang, L. Sun, and X. Zhang. 2013. Identification and characterization of genes that control fat deposition in chickens. **Journal of Animal Science and Biotechnology** 4(1):43. https://doi.org/ 10.1186/2049-1891-4-43.

Dai, D., F. Kong, H. Han, W. Shi, H. Song, I. Yoon, S. Wang, X. Liu, N. Lu, W. Wang, and S. Li. 2024. Effects of postbiotic products from Saccharomyces cerevisiae fermentation on lactation performance, antioxidant capacity, and blood immunity in transition dairy cows. **Journal of Dairy Science** 107(12):10584-10598. https://doi.org/10.3168/jds.2023-24435.

Dupont, J., M. Reverchon, L. Cloix, P. Froment, and C. Rame. 2012. Involvement of adipokines, AMPK, PI3K and the PPAR signaling pathways in ovarian follicle development and cancer. **International Journal of Developmental Biology** 56(10-11-12):959-967. https://doi.org/10.1387/ijdb.120134jd.

He, A., J. M. Dean, D. Lu, Y. Chen, and I. J. Lodhi. 2020. Hepatic peroxisomal β-oxidation suppresses lipophagy via RPTOR acetylation and MTOR activation. **Autophagy** 16(9):1727-1728. https://doi.org/10.1080/15548627.2020.1797288.

Hernandez, D., D. Nydam, S. Godden, L. Bristol, A. Kryzer, J. Ranum, and D. Schaefer. 2016. Brix refractometry in serum as a measure of failure of passive transfer compared to measured immunoglobulin G and total protein by refractometry in serum from dairy calves. **The Veterinary Journal** 211:82-87. https://doi.org/10.1016/j.tvjl.2015.11.004.

Hong, C., R. Deng, P. Wang, X. Lu, X. Zhao, X. Wang, R. Cai, and J. Lin. 2021. LIPG: an inflammation and cancer modulator. **Cancer Gene Therapy** 28(1):27-32. https://doi.org/10.1038/s41417-020-0188-5.

Huang, H., A. Lennikov, M. S. Saddala, D. Gozal, D. J. Grab, A. Khalyfa, and L. Fan. 2019. Placental growth factor negatively regulates retinal endothelial cell barrier function through suppression of glucose-6-phosphate dehydrogenase and antioxidant defense systems. **The FASEB Journal** 33(12):13695-13709. https://doi.org/10.1096/fj.201901353R.

Huang, J., R. Zhu, and D. Shi. 2021. The role of FATP1 in lipid accumulation: a review. **Molecular and Cellular Biochemistry** 476(4):1897-1903. https://doi.org/10.1007/s11010-021-04057-w.

Izuddin, W. I., A. M. Humam, T. C. Loh, H. L. Foo, and A. A. Samsudin. 2020. Dietary postbiotic Lactobacillus plantarum improves serum and ruminal antioxidant activity and upregulates hepatic antioxidant enzymes and ruminal barrier function in post-weaning lambs. **Antioxidants** 9(3):250. https://doi.org/10.3390/antiox9030250.

Ke, S., Z. Liu, Q. Wang, G. Zhai, H. Shao, X. Yu, and J. Guo. 2022. FAM107A Inactivation Associated with Promoter Methylation Affects Prostate Cancer Progression through the FAK/PI3K/AKT Pathway. **Cancers** 14(16), 3915. https://doi.org/10.3390/cancers14163915.

Kim, D., B. Langmead, and S. L. Salzberg. 2015. HISAT: a fast spliced aligner with low memory requirements. **Nature Methods** 12(4):357-360. https://doi.org/10.1038/nmeth.3317.

Kim, M., K. W. Park, Y. Ahn, E. B. Lim, S. H. Kwak, A. Randy, N. J. Song, K. S. Park, C. W. Nho, and Y. S. Cho. 2022. Genetic association-based functional analysis detects HOGA1 as a potential gene involved in fat accumulation. **Frontiers in Genetics** 13:951025. https://doi.org/10.3389/fgene.2022.951025.

Kutlu, O., H. N. Kaleli, and E. Ozer. 2018. Molecular pathogenesis of nonalcoholic steatohepatitis-(NASH-) related hepatocellular carcinoma. **Canadian Journal of Gastroenterology and Hepatology** 2018(1):8543763. https://doi.org/10.1155/2018/8543763.

Laarman, A. H., A. L. Ruiz-Sanchez, T. Sugino, L. L. Guan, and M. Oba. 2012. Effects of feeding a calf starter on molecular adaptations in the ruminal epithelium and liver of Holstein dairy calves. **Journal of Dairy Science** 95(5):2585-2594. https://doi.org/10.3168/jds.2011-4788.

Langmead, B. and S. L. Salzberg. 2012. Fast gapped-read alignment with Bowtie 2. Nature Methods 9(4):357-359. https://doi.org/10.1038/nmeth.1923.

Lee, Y. K., S. Y. Lee, J. R. Park, R. J. Kim, S. R. Kim, K. J. Roh, and J. S. Nam. 2012. Dysadherin expression promotes the motility and survival of human breast cancer cells by AKT activation. **Cancer Science** 103(7):1280-1289. https://doi.org/10.1111/j.1349-7006.2012.02302.x.

Li, B. and C. N. Dewey. 2011. RSEM: accurate transcript quantification from RNA-Seq data with or without a reference genome. **BMC Bioinformatics** 12:1-16. https://doi.org/10.1186/1471-2105-12-323.

Love, M. I., W. Huber, and S. Anders. 2014. Moderated estimation of fold change and dispersion for RNA-seq data with DESeq2. **Genome Biology** 15:1-21. https://doi.org/10.1186/s13059-014-0550-8.

Lubarski-Gotliv, I., C. Asher, L. A. Dada, and H. Garty. 2016. FXYD5 Protein Has a Pro-inflammatory Role in Epithelial Cells. **Journal of Biological Chemistry** 291(21):11072-11082. https://doi.org/10.1074/jbc.M115.699041.

Malone, J. H. and B. Oliver. 2011. Microarrays, deep sequencing and the true measure of the transcriptome. **BMC Biology** 9(1):34. https://doi.org/10.1186/1741-7007-9-34.

Manigandan, S., S. Mukherjee, and J. W. Yun. 2021. Loss of family with sequence similarity 107, member A (FAM107A) induces browning in 3T3-L1 adipocytes. **Archives of Biochemistry and Biophysics** 704:108885. https://doi.org/10.1016/j.abb.2021.108885.

McNeil, B., D. Renaud, M. Steele, L. Cangiano, M. Olmeda, C. Villot, E. Chevaux, J. Yu, L. Hernandez, and W. Frizzarini. 2024. Effects of weaning and inactivated Lactobacillus helveticus supplementation on dairy calf behavioral and physiological indicators of affective state. **Journal of Dairy Science** 107(12):11363-11380. 10.3168/jds.2023-24581.

Miller, T. J. and P. B. Davis. 2008. FXYD5 modulates Na+ absorption and is increased in cystic fibrosis airway epithelia. **American Journal of Physiology-Lung Cellular and Molecular Physiology** 294(4):L654-L664. https://doi.org/10.1152/ajplung.00430.2007.

Ming, F. and D. Zhang. 2025. FAM107A Inhibits the Growth, Invasion and Aerobic Glycolysis of LUAD Cells by Regulating CRYAB/PI3K/AKT. **Biochemical Genetics**:1-15. https://doi.org/10.1007/s10528-024-11006-x.

Nafikov, R. A., J. P. Schoonmaker, K. T. Korn, K. Noack, D. J. Garrick, K. J. Koehler, J. Minick-Bormann, J. M. Reecy, D. E. Spurlock, and D. C. Beitz. 2013. Association of polymorphisms in solute carrier family 27, isoform A6 (SLC27A6) and fatty acid-binding protein-3 and fatty acid-binding protein-4 (FABP3 and FABP4) with fatty acid composition of bovine milk. **Journal of Dairy Science** 96(9):6007-6021. https://doi.org/10.3168/jds.2013-6703.

Nakagawa, Y., A. Satoh, H. Tezuka, S.-i. Han, K. Takei, H. Iwasaki, S. Yatoh, N. Yahagi, H. Suzuki, Y. Iwasaki, H. Sone, T. Matsuzaka, N. Yamada, and H. Shimano. 2016. CREB3L3 controls fatty acid oxidation and ketogenesis in synergy with PPARα. **Scientific Reports** 6(1):39182. https://doi.org/10.1038/srep39182.

Pavlakis, E., R. Chiotaki, and G. Chalepakis. 2011. The role of Fras1/Frem proteins in the structure and function of basement membrane. **The International Journal of Biochemistry & Cell Biology** 43(4):487-495. https://doi.org/10.1016/j.biocel.2010.12.016.

Ríus, A. G., J. D. Kaufman, M. M. Li, M. D. Hanigan, and I. R. Ipharraguerre. 2022. Physiological responses of Holstein calves to heat stress and dietary

supplementation with a postbiotic from Aspergillus oryzae. **Scientific Reports** 12(1):1587. https://doi.org/10.1038/s41598-022-05505-3.

Salminen, S., M. C. Collado, A. Endo, C. Hill, S. Lebeer, E. M. Quigley, M. E. Sanders, R. Shamir, J. R. Swann, and H. Szajewska. 2021. The International Scientific Association of Probiotics and Prebiotics (ISAPP) consensus statement on the definition and scope of postbiotics. **Nature Reviews Gastroenterology & Hepatology** 18(9):649-667. https://doi.org/10.1038/s41575-021-00440-6.

Schüler, Y., C. Lee-Thedieck, K. Geiger, T. Kaiser, Y. Ino, W. K. Aicher, and G. Klein. 2012. Osteoblast-secreted factors enhance the expression of dysadherin and CCL2-dependent migration of renal carcinoma cells. **International Journal of Cancer** 130(2):288-299. https://doi.org/10.1002/ijc.25981.

Shi, B., J. Chen, H. Guo, X. Shi, Q. Tai, G. Chen, H. Yao, X. Mi, R. Zhong, Y. Lu, Y. Zhao, L. Sun, D. Zhou, Y. Yao, and S. He. 2025. ACOX1 activates autophagy via the ROS/mTOR pathway to suppress proliferation and migration of colorectal cancer. **Scientific Reports** 15(1):2992. https://doi.org/10.1038/s41598-025-87728-8.

Shimamura, T., J. Yasuda, Y. Ino, M. Gotoh, A. Tsuchiya, A. Nakajima, M. Sakamoto, Y. Kanai, and S. Hirohashi. 2004. Dysadherin expression facilitates cell motility and metastatic potential of human pancreatic cancer cells. **Cancer Research** 64(19):6989-6995. https://doi.org/10.1158/0008-5472.CAN-04-1166.

Sirisopapong, M., T. Shimosato, S. Okrathok, and S. Khempaka. 2023. Assessment of lactic acid bacteria isolated from the chicken digestive tract for potential use as poultry probiotics. **Animal Bioscience** 36(8):1209. https://doi.org/10.5713/ab.22.0455.

Song, L., X. Li, Q. Sun, and Y. Zhao. 2022. Fxyd5 activates the NF-**K**B pathway and is involved in chondrocytes inflammation and extracellular matrix degradation. **Molecular Medicine Reports** 25(4):134. https://doi.org/10.3892/mmr.2022.12650.

Stefańska, B., F. Katzer, B. Golińska, P. Sobolewska, S. Smulski, A. Frankiewicz, and W. Nowak. 2022. Different methods of eubiotic feed additive provision affect the health, performance, fermentation, and metabolic status of dairy calves during

the preweaning period. **BMC Veterinary Research** 18(1):138. https://doi.org/10.1186/s12917-022-03239-y.

Strauss, J. G., M. Hayn, R. Zechner, S. Levak-Frank, and S. Frank. 2003. Fatty acids liberated from high-density lipoprotein phospholipids by endothelial-derived lipase are incorporated into lipids in HepG2 cells. **Biochemical Journal** 371(3):981-988. https://doi.org/10.1042/bj20021437.

Szkopińska, A. and D. Płochocka. 2005. Farnesyl diphosphate synthase; regulation of product specificity. **Acta Biochimica Polonica** 52(1):45-55. https://doi.org/10.18388/abp.2005_3485.

Thorsteinsson, M. M., N. Canibe, and M. Vestergaard. 2020. Effect of dietary supplementation of Saccharomyces cerevisiae and a postbiotic from Lactobacillus acidophilus on the concentration of organic acids, biogenic amines, and microbiota in the small intestine and colon of rosé veal calves. **Journal of Animal and Feed Sciences** 29(4):345-351. https://doi.org/10.22358/jafs/131078/2020.

Tsukagoshi, M., M. Sirisopapong, F. Namai, M. Ishida, S. Okrathok, S. Shigemori, T. Ogita, T. Sato, S. Khempaka, and T. Shimosato. 2020. Lactobacillus ingluviei C37 from chicken inhibits inflammation in LPS-stimulated mouse macrophages. **Animal Science Journal** 91(1):e13436. https://doi.org/10.1111/asj.13436.

Van Niekerk, J., M. Middeldorp, L. Guan, and M. Steele. 2021. Preweaning to postweaning rumen papillae structural growth, ruminal fermentation characteristics, and acute-phase proteins in calves. **Journal of Dairy Science** 104(3):3632-3645. https://doi.org/10.3168/jds.2020-19003.

Wang, Z., J. Hu, W. Zheng, T. Yang, X. Wang, C. Xie, and X. Yan. 2019. Lactobacillus frumenti mediates energy production via fatty acid β-oxidation in the liver of early-weaned piglets. **Journal of Animal Science and Biotechnology** 10(1):95. https://doi.org/10.1186/s40104-019-0399-5.

Winkler, B. S., N. DeSantis, and F. Solomon. 1986. Multiple NADPH-producing pathways control glutathione (GSH) content in retina. **Experimental Eye Research** 43(5):829-847. https://doi.org/10.1016/S0014-4835(86)80013-6.

Xu, X., J. Chang, P. Wang, C. Liu, M. Liu, T. Zhou, Q. Yin, and G. Yan. 2022. Glycyrrhizic acid and compound probiotics supplementation alters the intestinal transcriptome and microbiome of weaned piglets exposed to deoxynivalenol. **Toxins** 14(12):856. https://doi.org/10.3390/toxins14120856.

Ye, F., Z.-d. Deng, K.-y. Liu, X.-m. Yao, W.-x. Zheng, Q. Yin, X. Hai, J.-k. Gan, Z.-F. Zhang, Z. Ma, and H. Li. 2024. Integrative analysis of the transcriptome, proteomics and metabolomics reveals key genes involved in the regulation of breast muscle metabolites in capons. **BMC Genomics** 25(1):1239. https://doi.org/10.1186/s12864-024-11142-z.

Zang, R., R. Zhou, Y. Li, H. Wu, L. Lu, and H. Xu. 2024. The probiotic Lactobacillus plantarum alleviates colitis by modulating gut microflora to activate PPARγ and inhibit MAPKs/NF-**K**B. **European Journal of Nutrition** 64(1):32. https://doi.org/10.1007/s00394-024-03520-w.

Zhang, H., Z. Shen, Z. Yang, H. Jiang, S. Chu, Y. Mao, M. Li, Z. Chen, A. Aboragah, and J. J. Loor. 2021. Abundance of solute carrier family 27 member 6 (SLC27A6) in the bovine mammary gland alters fatty acid metabolism. **Food & Function** 12(11):4909-4920. https://doi.org/10.1039/D0FO03289A.

Zhou, M. C., P. Yu, Q. Sun, and Y. X. Li. 2016. Expression profiling analysis: Uncoupling protein 2 deficiency improves hepatic glucose, lipid profiles and insulin sensitivity in high-fat diet-fed mice by modulating expression of genes in peroxisome proliferator-activated receptor signaling pathway. **Journal of Diabetes Investigation** 7(2):179-189. https://doi.org/10.1111/jdi.12402.

Zhou, X., H. Hadiatullah, T. Guo, Y. Yao, C. Li, and X. Wang. 2021. Dairy Processing Affects the Gut Digestion and Microecology by Changing the Structure and Composition of Milk Fat Globules. **Journal of Agricultural and Food Chemistry** 69(35):10194-10205. https://doi.org/10.1021/acs.jafc.1c04482.

Zhu, S., B. Zhang, T. Zhu, D. Wang, C. Liu, Y. Liu, Y. He, W. Liang, W. Li, R. Han, D. Li, F. Yan, Y. Tian, G. Li, X. Kang, Z. Li, R. Jiang, and G. Sun. 2023. miR-128-3p inhibits intramuscular adipocytes differentiation in chickens by downregulating FDPS. **BMC Genomics** 24(1):540. https://doi.org/10.1186/s12864-023-09649-y.